Full title

Environment-driven genomic and trait divergence in a neotropical mangrove highlight differential sensitivities to climate change

Short title

Environment-driven genomic and trait divergence in a non-model species

Authors

Mariana Vargas Cruz[1], Gustavo Maruyama Mori[2], Caroline Signori Müller[1], Carla Cristina da Silva[1], Dong-Ha Oh[3], Maheshi Dassanayake[3], Maria Imaculada Zucchi[4], Rafael Silva Oliveira[1] and Anete Pereira de Souza[1]*.

Affiliations

[1] Department of Plant Biology, Institute of Biology, University of Campinas, Campinas, São Paulo, Brazil.

[2]Institute of Biosciences, São Paulo State University (Unesp), São Vicente, São Paulo, Brazil.

[3]Department of Biological Sciences, Louisiana State University, Louisiana, United States.

[4]São Paulo Agency for Agribusiness Technology, Piracicaba, São Paulo, Brazil.

*Corresponding author. Email: anete@unicamp.br

Abstract

Integrating genomic and ecological data are instrumental for understanding the mechanisms of adaptive processes in natural ecosystems. In non-model species, such studies can be particularly challenging, but often brings to light results with implications for conservation. Here, we integrate molecular and ecophysiological approaches to assess the role of selection in the north-south organization of the genetic variation in the mangrove species *Avicennia schaueriana*, a new-world tree found from tropical to temperate coastal forests in the Atlantic coast of the Americas. In a common garden experiment, individuals from equatorial and subtropical forests diverged in traits involved in water balance and carbon acquisition, suggesting a genetic basis of the observed differences. RNA-sequencing highlighted the molecular effects of different light, temperature and air humidity in individuals under field conditions at contrasting latitudes. Additionally, genetic polymorphisms in trees sampled along most of the species range showed signatures of selection in sequences associated with the biogenesis of the photosynthetic apparatus, anthocyanin biosynthesis and osmotic and hypoxia stress responses. We found substantial divergences between populations occurring north and south of the north-eastern extremity of South America, underpinning roles of contrasting environmental forces in shaping the genetic structure of the species. The observed functional divergence might differentially affect sensitivities of populations to our changing climate, as discussed here. We indicate the necessity of independent conservation management for the long-term persistence of the species diversity. Moreover, we demonstrate the power of using a multidisciplinary approach in adaptation studies of non-model species.

1. Introduction

Adaptation to contrasting environments is an ubiquitous consequence of divergent selective forces acting on phenotypic diversity within species[1–3]. Phenotypic variation can be achieved through plasticity during acclimation to environmental changes, or ultimately through genetic variation shaped by adaptive processes[4]. Though the occurrence of intraspecific divergence in adaptive traits is well recognised, its molecular basis is not yet fully understood[5]. The integration of multiple independent approaches to understand the bases of adaptive trait variation is desirable to minimise the potential for incorrect conclusions[6].

In addition to its fundamental relevance in the field of evolutionary biology, research on the molecular mechanisms underlying adaptive variation has the potential to provide valuable information for ensuring species diversity persists under environmental challenges. Especially, accelerated rates of contemporary climate change call for studies on patterns of functional variation and its consequences for species responses to future climate conditions[7]. Climate change forecasts include a rise in sea-level from 0.26 to 0.82 m, an increase in mean atmospheric temperature from 0.3 to 4.8 °C and changes in precipitation regimes by the end of this century[8]. These changes are projected to especially affect certain ecosystems, as mangrove forests[9], since they are distributed in narrow intertidal environments in tropical and subtropical zones and are naturally limited by annual minimum temperatures and average rainfall[10]. Recent changes in sea level, in atmospheric temperature and in rainfall have already promoted shifts in the distribution of these ecosystems and in the density of individuals in forests[11–17]. Negative impacts are predicted mainly in regions in which aridity is expected to increase and where adjacent areas for population expansion are unavailable or do not exist[18]. However, in some regions,

mangroves are expected to persist through their ability to adjust soil elevation[11,19] and to rapidly shift their distribution to new suitable areas[11,18,20,21].

Yet, these predictions do not account for extant intraspecific variability across the geographical distribution of a given mangrove species. For instance, the genetic diversity of all mangrove species studied to date is structured into two populations occurring north and south of the northeast extremity of South America (NEESA)[22–24]. In the NEESA region, a bifurcating subdivision of the "South Equatorial Current" into the coastal "Guiana Current" and "Brazil Current" is observed, dispersing mangrove propagules in opposite directions and likely reducing the gene flow between populations[22,23,25] (Fig 1). Limited gene flow is a key process determining the magnitude of local adaptation and, when this condition is met, one may expect populations to adapt differently to their environments[2,26]. However, the neutral nature of the molecular markers used in previous works[22,23,25] precluded inferences on environment-driven genetic divergence.

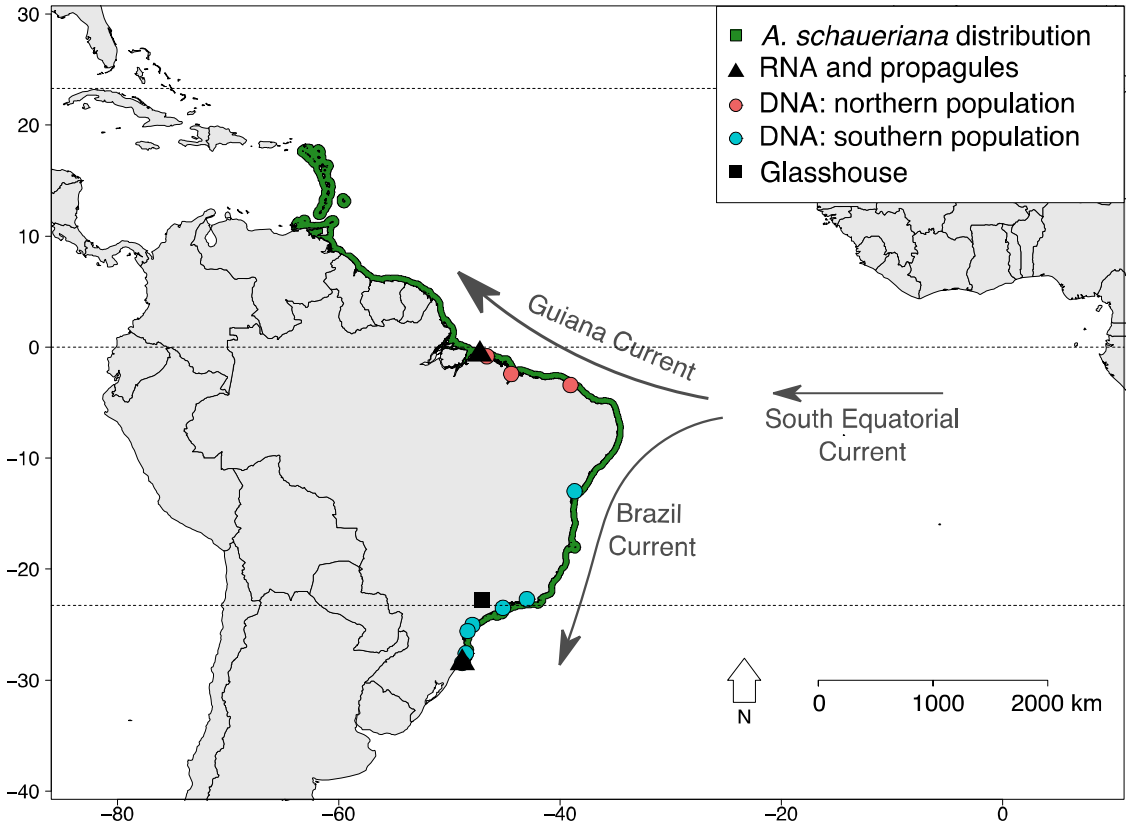

Fig 1. Geographical location of *Avicennia schaueriana* sampling sites. The green shaded area represents the geographical distribution of the species. Black triangles represent the location of the Equatorial and Subtropical sampling sites for propagules and plant tissues used in the common garden experiment and in RNA-sequencing, respectively. Coloured dots represent sampling sites of leaves used for extraction of genomic DNA for nextRAD sequencing (red: population located north of the northeast extremity of South America (NEESA); blue: population located south of the NEESA). Arrows approximately represent the direction of the major sea currents that act along the Atlantic coast of South America.

Advances in DNA sequencing now permit the undertaking of genome-wide studies to identify neutral and putatively adaptive genetic variation even in non-model organisms, such as mangrove trees[27]. We used these tools in the present work to investigate the non-neutral divergence between previously identified populations of the new-world mangrove tree *Avicennia schaueriana* Stapf & Leechman ex Moldenke. We further explored the potential role of environmental forces underlying such divergence along the Atlantic coast of South America. *Avicennia schaueriana* is the most widely distributed mangrove species with genetic diversity information available over this geographic scale. The species is found in the

92 Lesser Antilles (~16 °N) and from Venezuela to the southernmost mangrove forests in the
93 Atlantic (~28 °S)[28]. To avoid incorrect conclusions about the targets of selection[6], we
94 integrated three independent but complementary molecular and ecological approaches: (1)
95 comparative physiology of contrasting Equatorial and Subtropical samples grown in a
96 common garden experiment; (2) comparative transcriptomics of trees from Equatorial and
97 Subtropical localities, sampled in their native environments (Table 1, S1 Fig) and (3) genome
98 scans for signatures of selection using high-throughput genome-wide genotyping of
99 individuals, sampled along almost the entire distribution of the species (Fig 1). We further
100 discuss the implications of our results in the face of predicted changes in climate as well as
101 potential strategies for mangrove conservation along the Atlantic coast of South America.
102
103 **Table 1.** Characterisation of Subtropical and Equatorial sampling sites of propagules used in the
104 common garden experiment and of RNA used for RNA-sequencing.

Environmental features	Subtropical	Equatorial
Köppen-Geiger climate characterisation[†]	Temperate oceanic with hot summer, without a dry season (Cfa)	Tropical monsoon (Am)
Latitude	28 S	0
Tidal amplitude	Microtidal (< 1 m)	Macrotidal (> 4 m)
Annual mean temperature (°C)[‡]	20.09	26.42
Minimum temperature of the coldest month (°C)[‡]	11.76	22.04
Maximum temperature of the warmest month (°C)[‡]	28.66	31.1
Annual precipitation (mm)[‡]	1,435	2,216
Precipitation in the driest month (mm)[‡]	88	4
Precipitation in the wettest month (mm)[‡]	162	452
Mean air VPD (KPa)[‡]	1.95	2.82
Maximum air VPD (KPa)[‡]	2.47	2.95

Minimum air VPD (KPa)[‡]	1.48	2.71
Mean irradiance (KJ m^{-2} day^{-1})[‡]	14,270	17,414
Maximum irradiance (KJ m^{-2} day^{-1})[‡]	20,802	21,671
Minimum irradiance (KJ m^{-2} day^{-1})[‡]	8,201	13,874
Mean sea surface salinity (g/kg)[§]	35.50	34.96
Sea surface salinity in the saltiest month (g/kg)[§]	36.24	36.87
Sea surface salinity in the freshest month (g/kg)[§]	33.73	32.54
Average day length (hours (± sd))[¶]	12.103 (±1.251)	12.115 (±0.033)
True mangrove species at this area	*Avicennia schaueriana* *Laguncularia racemosa*	*Avicennia germinans* *Avicennia schaueriana* *Laguncularia racemosa* *Rhizophora mangle* *Rhizophora racemosa* *Rhizophora harriisoni*

VPD: Vapour pressure deficit. [†]According to Alvares *et al.* [114]. [‡]Source: BioClim[31]. [§]Source: MARSPEC[32]. [¶]Source: 'daylength' function from R package 'geosphere'[115]. sd: standard deviation of the mean.

2. Results

2.1 Comparative physiology in a common garden experiment

To identify functional divergence between individuals from Equatorial and Subtropical sites, we conducted a common garden experiment in a glasshouse, under a homogeneous, non-climate-controlled environment. We observed differences in key morphophysiological traits between seedlings from contrasting latitudes grown in this experiment (Fig 2 and 3). Subtropical plants showed higher transpiration rates and stomatal conductance than Equatorial plants (S2 Fig). Additionally, plants from the two origins were morphologically different from each other. The inclination angle of the leaf lamina was steeper in Equatorial than Subtropical plants, and the average size of individual leaves was smaller in Equatorial seedlings, even though the total leaf area and specific leaf area did not significantly differ between the groups (Fig 2, S1 Table, S3 Fig, S1 Data). Subtropical plants

accumulated more biomass in all vegetative organs (leaves, stems and roots) in comparison to Equatorial plants under the experimental conditions. However, the biomass fraction allocated to stems in relation to other organs (stem dry mass ratio, SMR = stem dry biomass/plant dry biomass) was greater in Equatorial plants, whereas allocation to leaves (leaf dry mass ratio, LMR = leaf dry biomass/plant dry biomass) was greater in Subtropical plants. Biomass allocation to roots (root dry mass ratio, RMR = root dry biomass/plant dry biomass) did not differ between groups (S1 Table). Unexpectedly, 63% of the Equatorial plants flowered after the sixth month of growth (S3G Fig). Since this was not observed in any Subtropical plant, Equatorial plants with reproductive branches were not used in the biomass allocation analysis.

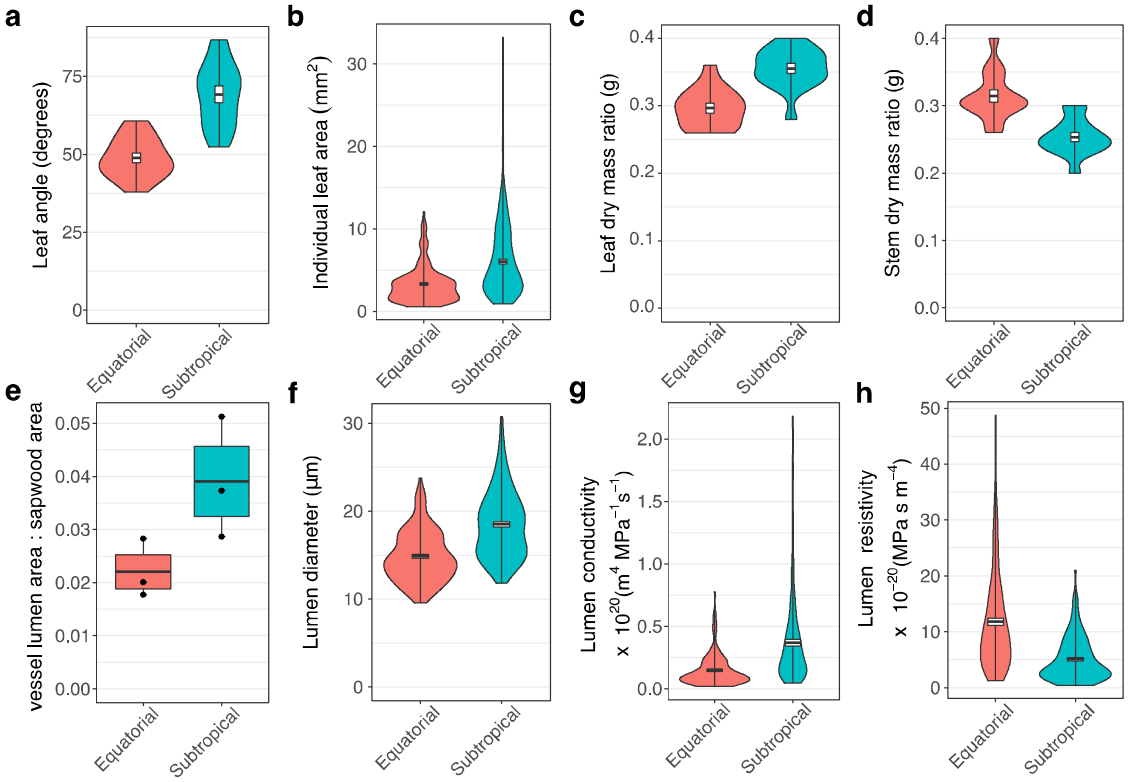

Fig 2. Morphological divergence observed in seedlings of *Avicennia schaueriana* collected from an Equatorial and a Subtropical sampling sites and grown in a glasshouse conducted common garden experiment. Violin plots represent the distribution of observations for plants from Equatorial (red) and Subtropical (blue) sampling sites. Box plots represent the mean, standard error, maximum and minimum values. Two group comparisons were performed using the non-parametric unpaired Mann-Whitney Wilcoxon U-tests. For all variables represented in the figure, the absence of a difference between groups was rejected at a significance threshold of 0.05. (A) Leaf inclination angle

(n = 15 leaves per group, 5 plants per group); (B) individual leaf area (n = 250 leaves per group, 3 plants per group); (C) leaf dry mass ratio (Leaf dry biomass/Plant dry biomass) (n = 15 plants per group); (D) stem dry mass ratio (Stem dry biomass/Plant dry biomass) (n = 15 plants per group); (E) vessel lumen area ratio in sapwood (n = 175 per group, 3 plants per group, observations represented by black points); (F) vessel lumen diameter (n = 700 vessels per group, 3 plants per group); (G) vessel lumen conductivity (n = 700 vessels per group, 3 plants per group); (H) vessel lumen resistivity (n = 700 vessels per group, 3 plants per group).

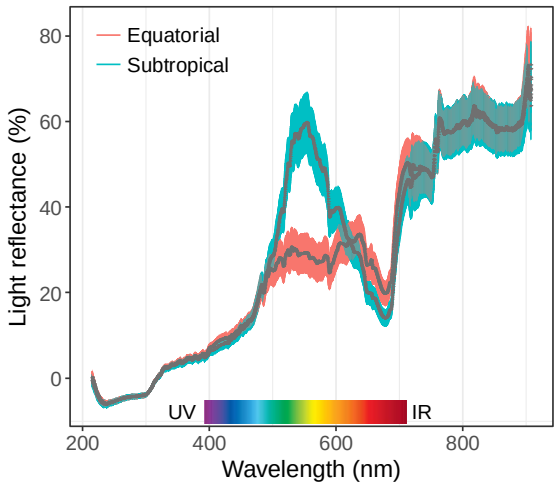

Fig 3. Light reflectance of the stem epidermis of five-month-old *Avicennia schaueriana* seedlings grown in a common garden experiment. Grey lines represent the mean reflectance and colour-shaded areas represent the standard error for each seedling source site (red: Equatorial; blue: Subtropical, n = 10 plants per group). The visible light spectrum range is highlighted in the figure.

Stems from Subtropical samples showed wider vessel lumen diameter than those from Equatorial samples, but the vessel density was not significantly different between the groups (Fig 2, S3H-S3I Fig). The sapwood space dedicated to vessel lumen area was also greater in Subtropical than in Equatorial plants. Vessels of Subtropical plants, showed higher conductivity at a detriment of hydraulic safety, compared to Equatorial plants (Fig 2). The total conductivity of the stems was not significantly different between the sampling groups. Additionally, plants from these contrasting origins exhibited different pigmentation in the stem epidermis. Stems from Equatorial seedlings reflected more red light of long wavelengths (635-700 nm) and less green light of medium wavelengths (520-560 nm) than Subtropical seedlings (Fig 3, S2 Data).

2.2 Comparative transcriptomics using an RNA-sequencing experiment

In the absence of a reference genome, we used RNA-sequencing (RNA-Seq)[55] to obtain a *de novo* assembled transcriptome for *A. schaueriana* from leaves, stems and flowers of six adult individuals, from Equatorial and Subtropical sampling sites (S4 Fig). We obtained over 240 million raw, paired-end, 72 bp reads and over 209 million high quality reads after quality control (Fig 1, Table 2). High quality reads were assembled into 49,490 transcripts of the species, after the removal of misassembled, contaminant and redundant transcripts. Putative protein-coding sequences comprised 61% of the transcriptome (30,227 sequences). Over 91.9% of the high-quality reads were mapped to a single transcript, providing evidence of minimum redundancy and a wide representation of reads obtained via sequencing (S2 Table). Moreover, searching for universal plant orthologous genes using the BUSCO pipeline[45] revealed that 91.8% of the conserved sequences in the plant database were present in the reference transcriptome (S2 Table). Assembled sequences with complete ORF represented approximately 42% (12,796) of all putative protein-coding transcripts, with an average length of 1,324 nucleotides (S3 Table, S5 Fig). The majority (94.33%) of these putative protein-coding sequences showed significant similarity to proteins in the Plant RefSeq[40] and TAIR databases. Only a minor fraction (2.85%) of the putative protein-coding transcripts could not be annotated using publicly available databases (S5C Fig). More than 80% of transcripts matched proteins from *Sesamum indicum* L. or *Erythranthe guttata* (Fisch. ex DC.) G.L. Nesom, which, together with *A. schaueriana* are grouped in the order Lamiales (S5D Fig). We identified putative orthologous genes between *A. schaueriana* and other closely related *Avicennia* L. (Avicenniaceae) species. This analysis revealed the presence of 27,658, 18,325 and 13,273 putative orthologues between the *A. schaueriana*

reference transcriptome and the transcriptomes derived, respectively, from *A. marina*[56] leaves and *A. officinalis* leaves[57] and roots[58] (S4 Table).

Table 2. Characterisation of field conditions at the moment of plant material collection and storage in RNA-stabilizing solution for subsequent sequencing.

Sample ID	Sampling site (Climate†)	GPS Point	Date (d/m)	Time (h:m)	TL (m)	DL (h)	Temp (°C) ‡	RH (%)‡	VPD (kPa) §	SI (KJ/m^2) ‡
St1	Subtropical (Cfa)	28.48 S; 48.88 W	23/08	15:15	0.5	11.3	19	84	0.351	2033.89
St2	Subtropical (Cfa)	28.36 S; 48.80 W	24/08	10:35	0.5	11.3	18.3	86	0.294	1804.15
St4	Subtropical (Cfa)	28.48 S; 48.83 W	25/08	13:11	0.5	11.3	20.9	82	0.445	1863.14
Eq4	Equatorial (Am)	00.64 S; 47.26 W	28/07	11:57	2.7	12.1	28.5	49	1.983	1940.73
Eq5	Equatorial (Am)	00.65 S; 47.26 W	29/07	12:22	2.7	12.1	28.3	51	1.883	2724.54
Eq6	Equatorial (Am)	00.64 S; 47.26 W	29/07	16:04	0.7	12.1	30.1	47	2.260	1433.68

TL: Tidal level; DL: day length; Temp: atmospheric air temperature; RH: atmospheric relative humidity; VPD: air vapour pressure deficit; SI: solar irradiance.
†Köppen-Geiger Climate classification according to Alvares *et al.*[114].
‡Source: Brazilian National Institute of Meteorology (INMET).
§Estimated according to McRae[116].

To identify environmental forces associated with variations in gene expression between source sites, we detected differentially expressed transcripts (DET) between samples using the EdgeR[46]. Sampling was conducted at the end of winter at the Subtropical site and at the beginning of the dry season at the Equatorial site (Table 2). Although plant material was collected under uncontrolled field conditions, we observed a consistency in transcripts expression levels from leaves and stems samples from plants from the same sampling site (S6A-S6B Fig). Levels of transcript expression in flowers, however, did not present a consistent pattern within sampling sites (S6C Fig), leading to the identification of only one

DET between flowers from Equatorial and Subtropical sites. Therefore, we did not include flowers in the subsequent analyses (S6F Fig). Conversely, we identified 1,837 and 904 transcripts showing significantly different (FDR < 0.05) relative abundance, respectively in leaves and stems, between samples at the Equatorial and at the Subtropical sites (S6D-S6E Fig). Among the 2,741 DET, 1,150 (41.91%) were putative protein-coding transcripts.

The assignment of transcripts to Gene Ontology (GO) terms was possible for 25,184 (83.31%) out of 30,227 putative protein-coding sequences in the transcriptome and enabled the performing of GO enrichment analyses of the DET. GO analyses were focused on biological processes potentially regulating the responses of *A. schaueriana* trees to the contrasting climatic variables in the equatorial and subtropical regions (Table 1, S1 Fig). Analyses were conducted separately for leaves and stems and for each of the two sets of DET, one showing increased expression levels in Equatorial than in Subtropical samples (we refer to these as DET-Eq) and the other set showing higher abundance in Subtropical compared to Equatorial samples (these are referred as DET-St). The enriched processes among the sets of DET included photosynthesis, plant responses to UV, to temperature stimulus, to water stress, to cell wall biosynthesis and to cellular respiration (S5-S9 Tables, S6I-S6-L Fig).

2.2.1 Photosynthesis

Among the DET-St, we observed the enrichment of categories related to photosynthesis, including various putative genes participating in the biosynthesis of the photosynthetic apparatus, in the biosynthesis of chlorophyll and photoreceptors, in the function of electron transporters and in the coordination of chloroplasts movement. In contrast, the DET-Eq set showed enrichment in transcripts similar to proteins required for

disassembling the light-harvesting complex of photosystem II in thylakoid membranes and for triggering chlorophyll degradation[59] (S6I-S6J Fig, S9 Table).

2.2.2 Response to UV

Both DET-St and DET-Eq sets showed enrichment in functions related to the response to UV-light, however, the sets of UV-responsive genes differed between these groups. The DET-St included UV-B protectants and genes involved in the biosynthesis of antioxidants induced by UV-B, such as plastid copper/zinc superoxide dismutases, photosystem II repair proteins, and transcripts involved in the synthesis of the antioxidant L-ascorbic acid (vitamin C). Conversely, the set of DET-Eq showed enrichment of putative genes involved in photo-oxidative damage reduction and in the positive regulation of anthocyanin biosynthesis in response to UV light. Antioxidants induced by UV irradiation[60], such as iron superoxide dismutases and transcripts involved in the biosynthesis of the pyridoxine (vitamin B6), were also among the DET-Eq (S9 Table 9).

2.2.3 Response to temperature

In the DET-St set, we observed putative genes presenting critical roles in chloroplast protein translation during cold acclimation and which provide tolerance to chilling temperatures[61,62]. For instance, transcripts similar to the *GLYCINE-RICH RNA-BINDING PROTEIN* (*RZ1A*), which has a chaperone activity during cold acclimation[63], and to the ATP-dependent *DNA HELICASE* ATSGS1, a cold-inducible protein required for DNA damage-repair[64]. Interestingly, we also identified in the DET-St set a putative *AGAMOUS-LIKE 24* (*AGL24*) transcription factor, involved in floral transition induced by vernalisation[65]. Contrastingly, various transcripts similar to heat shock-inducible

chaperones and an *ADENINE NUCLEOTIDE ALPHA HYDROLASE-LIKE PROTEIN* (*AT3G53990*), involved in chaperone-mediated protein folding[66], were detected in the set of DET-Eq, potentially enhancing tolerance to heat in the Equatorial plants. Additionally, a transcript similar to the *ETHYLENE-RESPONSIVE ELEMENT BINDING PROTEIN* (*RAP2.3*), which confers resistance to heat and to hydrogen peroxide[67], was observed in this group (S9 Table).

2.2.4 Response to water stress

Transcripts associated with the response to water deprivation, to cellular ion homeostasis and to osmotic adjustment were enriched in the DET-Eq. Dehydration-induced transcriptional regulators and genes that improve tolerance to water deficits were among these transcripts. For instance, a transcript similar to the *ETHYLENE-RESPONSIVE TRANSCRIPTION FACTOR* (*RAP2.4*), induced by water stress and that regulates the expression of several drought-responsive genes, including aquaporins[68,69] was identified in the DET-Eq. Accordingly, a putative aquaporin *PLASMA MEMBRANE INTRINSIC PROTEIN (PIP1;4*)[70] was also in this set. We also observed in the DET-Eq, putative genes participating in the synthesis and accumulation of raffinose, an osmoprotective soluble trisaccharide[71], and also transcripts similar to osmosensitive ion channels belonging to the *EARLY-RESPONSIVE TO DEHYDRATION STRESS FAMILY PROTEIN*. In line with this, we observed among the DET-Eq an ion channel protein, *SLAC1 HOMOLOGUE 3* (*SLAH3*), required for stomatal closure induced by drought stress[72] and also the putative *NINE-CIS-EPOXYCAROTENOID DIOXYGENASE 3* (*NCED3*), which increases plant resistance to water deficit, through the accumulation of abscisic acid (ABA) leading to stomatal closure. Possibly as a consequence from decreased stomatal conductance, a transcript similar to the

274 *ALANINE-GLYOXYLATE AMINOTRANSFERASE 2 HOMOLOG 3* (*AT3G08860*), which
275 plays a central role in photorespiration[73], showed higher expression in Equatorial than in
276 Subtropical samples (S9 Table).
277
278 *2.2.5 Cell wall biosynthesis*
279 Transcripts similar to 33 distinct proteins and transcription factors that play central
280 roles in the biosynthesis and deposition of distinct cell wall components, such as cellulose,
281 hemicellulose, lignin and pectin, were identified among the DET-Eq (S9 Table).
282
283 *2.2.6 Cellular respiration*
284 The DET-Eq were also enriched in putative cellular respiration genes, which included
285 one enzyme encoded in the nuclear genome, the *ACONITASE 3* (*ACO3*), which converts
286 citrate to isocitrate in the tricarboxylic acid cycle (TCA cycle), and several other genes from
287 the mitochondrial genome, encoding subunits of the NADH dehydrogenase, of the ATP-
288 synthase and of the cytochrome C oxidase (S9 Table).
289 We verified and confirmed the results obtained in the computational analyses of RNA-
290 Seq data by qRT-PCR of 10 DET detected across all leaf samples (S7 Fig, S10 Table, S1
291 Result).
292
293 ***2.3 Detection of genetic variants with a signature of positive selection***
294 To complement the analyses of differential gene expression, which could result from
295 both plasticity and adaptive selection[74], we searched for gene sequence variation in trees
296 sampled along the Atlantic coast of South America (Fig 1, S11 Table). After quality filtering
297 of sequenced data, we selected 77 individuals, which did not show signs of interspecific

hybridization with *Avicennia germinans*, for downstream analyses. These data were used in population genetics approaches to describe genetic structure and to perform genome-scans for loci with signatures of positive selection. We identified a set of 6,170 high-quality unlinked biallelic single nucleotide polymorphic loci (SNP) with a minor allele frequency ≥ 0.05 and ≥ 8x coverage. The overall genetic structure corroborated a previous study based on putatively neutral microsatellite loci[22], dividing the sampling sites into two main groups: north and south of the NEESA (S8 Fig).

To investigate the role of non-neutral evolutionary forces driving the observed population divergence, we used two distinct methods that allowed the detection of loci that showed significant departures from a neutral expectation of interpopulation divergence. To minimise false-positive signatures of selection, we considered 122 loci that were conservatively detected by both pcadapt[54] and LOSITAN[75]. These loci were aligned to transcriptome characterised herein, enabling the screening for their potential functional roles. We found 16 candidate loci with putative evidence of selection within expressed sequences, 15 of which showed similarity to gene models in *A. thaliana* and *S. indicum* (S12 Table). However, five of these reference proteins did not have informative function described for the model plant, hindering inferences about their putative function in *A. schaueriana*. Conversely, among the remaining ten annotated candidate loci, we found five genes involved in processes related to the contrasting climate regimes of equatorial and subtropical environments. One of the candidate SNP loci was detected in the putative transcription factor *ETHYLENE-RESPONSIVE TRANSCRIPTION ACTIVATOR* (*RAP2.4*), which is induced in response to water and salt stress. This gene also regulates developmental processes mediated by light intensity[68] and the expression of aquaporins in *A. thaliana*[69], playing a role in plant water homeostasis. Two other candidate loci with putative signature of selection were associated

with transcription factors, the *ZINC-FINGER PROTEIN 1* (*ZFN1*), involved in the regulation of the expression of several water stress genes[76] and the *HYPOXIA RESPONSE ATTENUATOR* (*HRA1*)[77], which is strongly induced in *A. thaliana* in response to low oxygen levels. Additionally, the putative enzyme *UDP GLUCOSYL TRANSFERASE*, which catalyses the final step of anthocyanin biosynthesis, wherein pigmentation is produced[78], also showed a SNP variation with putative sign of positive selection. And one candidate locus was present in a transcript similar to the *AT2G20710* gene model in *A. thaliana*, a *TETRATRICOPEPTIDE REPEAT* (*TPR*) protein, which might play a role in the biogenesis of the photosynthetic apparatus[79].

2.4 Data availability statement

All relevant morphophysiological data assessed from plants grown in the common garden experiment are available in the Supplementary information files (S1-S2 Data). Expression data and sequences that support the findings have been deposited in GenBank with the primary accession code GSE116060. Variant Call Format (VCF) file and its complementary file, both required for all genome-wide SNP diversity analyses are available in the Supplementary information files (respectively S3 Data and S4 Data).

3. Discussion

In the present work, we used complementary ecological and molecular approaches to unveil the nature of non-neutral phenotypic and genetic divergences as well as the role played by contrasting environmental forces between two populations of the mangrove species, *Avicennia schaueriana*. The overall genetic structure previously detected with a few microsatellite loci between populations occurring north and south of the northeast extremity

of South America (NEESA)[22] was confirmed here using thousands of genome-wide SNP loci (S8 Fig). Additionally, a common garden experiment revealed morphophysiological differences in traits that are key to the regulation of water and carbon balances between seedlings originated from the Equatorial and Subtropical sampling sites (Fig 2-3). Comparatively, the Equatorial plants showed morphophysiological and transcriptomic signals that appear to minimise effects of low water, high light and heat stresses, whereas traits observed in Subtropical plants suggest a maximisation of carbon assimilation, beneficial especially under low temperature and reduced light regime.

Traits exhibited by Equatorial plants compared to Subtropical plants in the common garden experiment, such as reduced leaf size, the steeper leaf angle, higher levels of red light-reflecting pigments, narrower vessels and lower rates of stomatal conductance, limit carbon acquisition[80] and may have imposed constraints to carbon gain in Equatorial plants, which also accumulated less biomass (Fig 2-3, S2-S3 Fig). Conversely, such characteristics allow plants to maintain leaf temperature at suitable levels for photosynthesis, while reducing both UV-exposure, through protective pigmentation and leaf inclination, and water loss, through minimisation of evaporative cooling[80,81]. We argue that the prevalence of these traits among Equatorial individuals may be advantageous in their natural environment, especially during the dry season (from August to December), when high light intensity is frequently combined with high temperature (> 30 °C) and average air humidity below 70% (Table 1, S1 Fig). In the presence of high atmospheric evaporative demand and highly saline intertidal soils, water acquisition has an elevated energetic cost, representing a strong selective pressure in favour of water-saving adaptations[80]. Accordingly, Equatorial plants also showed lower transpiration rates than Subtropical plants in the common garden (S3 Fig). In addition, 63% of the Equatorial plants showed an early transition from vegetative to reproductive stage, starting

369 flowering after only sixth months of growth, in July and August (S3G Fig). The period in
370 which flowering occurred is concordant with observations reported in literature for the species
371 in tropical sites, from June-August [82], however we did not find records of six-months-old
372 flowering plants. Even though in southern subtropical forests, a flowering peak is also
373 observed in August[83], Subtropical plants did not flower during the experiment. Early
374 flowering is a phenotype with complex genetic components, rarely studied, especially in non-
375 model organisms, but is an important adaptive mechanism for maximizing the chances of
376 reproduction under stress[84].

377 In contrast, Subtropical plants showed higher stomatal conductance and transpiration
378 rates, higher levels of green light-reflecting pigments, larger leaf area, wider leaf lamina angle
379 and larger xylem vessel diameter than Equatorial plants in the common garden experiment
380 (Fig 2-3, S2-S3 Fig). These characteristics enhance light energy absorbance and carbon
381 acquisition at the expense of greater water loss and higher cavitation risk[85,86]. These traits
382 may also compensate for declines in net primary production in higher-latitude
383 environments[87], resulting from compressed environmental windows of opportunity, mainly
384 in terms of temperature and solar irradiance (Table 1, S1 Fig). We argue that the intensity of
385 cold events in southern Subtropical populations of *A. schaueriana* is likely not sufficiently
386 expressive to favour the selection of freezing-tolerant individuals, in contrast to results
387 reported for the congeneric *A. germinans* at its northernmost distribution limit, on the Atlantic
388 coast of North America[14]. At the southern range edge of *A. schaueriana*, the annual
389 minimum air temperature does not drop below 0 □ (Table 1, S1 Fig), thus being higher than
390 the expected mangrove physiological threshold[10]. Additionally, the relatively small
391 population size of *A. schaueriana* at this location[28] and the arrival of maladapted

392 propagules from northerly populations might reduce the potential strength of natural selection
393 in favour of cold-adapted individuals at this Subtropical site.

394 Functional interpopulation divergence was also evident under field conditions at the
395 molecular level. Comparative transcriptomics of trees sampled in field conditions corroborate
396 with the suggested effects of the environmental variation in light availability, temperature and
397 water stress on the phenotypic divergence observed in the common garden experiment.
398 Transcriptomic profiles were obtained at the beginning of the dry season in the Equatorial
399 sampling site and at the end of winter in the Subtropical sampling site (Table 2) and showed
400 an enrichment of DET involved in photosynthesis, cellular respiration, cell wall biosynthesis
401 and plant responses to water stress, temperature stimulus and UV light (S6I-S6L Fig).
402 Additionally, the adaptive relevance of these biological processes in the field was highlighted
403 through the identification and functional annotation of SNP loci putatively under natural
404 selection from populations along the *A. schaueriana* geographic distribution (S12 Table). In
405 the following subsections, we integrate information derived from these different methods.
406

407 ***3.1 Water stress as a relevant selective pressure in equatorial populations***

408 The increased levels of transcripts similar to heat-shock proteins, drought-induced ion
409 transporters, genes that enhance tolerance to heat, that are involved in stomatal closure and
410 that play central roles in photorespiration, provided multiple lines of evidence of water stress
411 in Equatorial samples. Additionally, compared to Subtropical plants, Equatorial plants
412 exhibited higher basal levels of expression of aquaporins and genes involved in the
413 accumulation of organic solutes. These investments improve tolerance to drought[71] by
414 lowering the cell water potential and rather actively transporting water through proteins in the
415 cell membrane than using passive apoplastic water transport[80,88,89]. The enhanced rigidity

of cells reduces the risk of cell damage during the dehydration and rehydration process and, thus, improves resistance to the high extra-cellular osmotic pressure[90]. Therefore, we argue that the higher expression of several transcripts similar to key secondary cell wall biosynthesis and cell wall thickening genes in Equatorial samples also suggests plant responses to water stress. Corroborating evidences of the relevance of water stress in the Equatorial environmental conditions, we identified gene sequence divergence between populations north and south of the NEESA in two putative osmotic stress-responsive regulatory transcription factors (*RAP2.4* and *ZFN1*), one of which also induces the expression of aquaporins (*RAP2.4*). These findings are additionally supported by the divergence in traits related to water balance between plants from Equatorial and Subtropical sampling sites, such as leaf size, vessel diameter, leaf angle and transpiration and stomatal conductance rates (Fig 2, S2 Fig).

3.2 Latitudinal variation in light quality and intensity may shape non-neutral diversity

Contrasting seasonal fluctuations in the photoperiod and in the light quality throughout the year between low and high latitudes[91] (Table 1) likely influence the differential expression of putative UV-inducible antioxidant and photodamage repair genes. The adaptive relevance of this is supported by the natural selection sign found in a transcript similar to a key gene to the biosynthesis of anthocyanin, which confers protection to UV-B irradiation (*UDP-GLUCOSYL TRANSFERASE*). Divergent morphological traits between Equatorial and Subtropical plants grown in the common garden experiment, including leaf inclination angle and stem light reflectance, corroborate with the observed differential gene expression and genomic signatures for positive selection (Fig 2 and 3).

3.3 Low water and low light availability may affect photosynthesis and cellular respiration

In response to abiotic stress conditions such as drought, heat and high light, plants optimise the use of light energy and minimise photooxidative damage, reducing the photosynthetic activity by repressing light-harvesting and photosystem-component genes[92–100]. We argue that the lower expression of photosynthesis genes in Equatorial than in Subtropical samples likely reinforces the relevance of water stress in shaping divergent phenotypes in the field, but also may result in an enhanced absorption of light energy in Subtropical plants. Accordingly, we identified an increased expression of transcripts associated with chlorophyll biosynthesis in the DET-St set and with chlorophyll breakdown and leaf senescence in the DET-Eq set. The degradation of chlorophyll followed by leaf senescence allows the remobilisation of nutrients and reduces the water loss through leaf transpiration, contributing to water balance and to drought tolerance[101]. In addition, we detected a putative genetic signature of selection in a transcript similar to a *TPR* protein, required for chlorophyll synthesis and for the biogenesis of the photosynthetic apparatus[79]. Thus, we suggest that differential seasonality in light and water availability at subtropical and equatorial latitudes may be involved in the divergence of non-neutral variability in the species. Corroborating with the genomic approaches, we observed divergence of functional traits related to water use and to the absorbance of light energy in plants from contrasting latitudes cultivated under the same environmental conditions (Fig 2-3, S2-S3 Fig).

The mitochondrial activity is deeply connected to the photosynthesis and to chloroplasts function since it generates ATP for carbohydrate synthesis, plays a role in the protection of chloroplasts against photoinhibition, participates in the dissipation of reducing equivalents and exchanges metabolites with chloroplasts during photorespiration[102,103].

464 Cellular respiration also provides ATP and carbon compounds for secondary metabolism,
465 playing a fundamental role in responses to abiotic stresses, including drought[102,104]. We
466 suggest that the higher levels of cellular respiration genes in Equatorial than in Subtropical
467 samples, may be a consequence of the reduced expression of photosynthesis genes and
468 enhanced energetic demand caused by water stress.
469
470 ***3.4 Tidal amplitude variation with latitude may act as a diverging force along the***
471 ***Atlantic coast of South America***
472 Tidal amplitude is markedly reduced with increasing latitude along the Atlantic coast
473 of South America, ranging from greater than 4 m at low latitudes to less than 1 m at high
474 latitudes[105]. The wide variation in tidal amplitude exposes trees to contrasting durations of
475 hypoxia. The identification of a candidate SNP locus with putative sign of positive selection
476 in a transcription factor induced by oxygen deprivation (*HRA1*) may indicate that differential
477 tidal variation act as a diverging selective force between northerly Equatorial and southerly
478 Subtropical populations of *A. schaueriana*. The *HRA1* putative homolog also showed a 1.75-
479 fold higher expression in Subtropical leaves relative to Equatorial leaves under field
480 conditions. However, we did not detect evidences at the phenotypic level in the common
481 garden experiment corroborating with the suggested relevance of this environmental variable.
482
483 ***3.5 Climate change and conservation implications of the results***
484 The functional divergence observed in this work might differentially affect the
485 sensitivity of populations of *A. schaueriana* to a rapidly changing climate. Although there is
486 no evidence of mangrove expansion at its southernmost range limit on the Atlantic coast of
487 South America[28], researchers suggest that populations could expand polewards in the near

488 future, benefitting from the increased air and ocean temperatures and greenhouse gas
489 concentrations[106]. We expect that the more acquisitive phenotypic traits exhibited in the
490 common garden experiment by *A. schaueriana* seedlings from the subtropical range edge may
491 indeed be favourable for growth under increased temperatures and rainfall[8]. However, due
492 to the low tidal variation (< 1 m) observed in the southernmost mangrove distribution edge in
493 the Atlantic coast of South America, a greater relocation of forests is required for trees to
494 keep pace with the rising sea-level[107]. In this context, dense human coastal occupations
495 combined with the narrow intertidal zones, characteristic of this region, make mangroves at
496 higher latitudes more vulnerable to habitat loss than in the equatorial region of the Atlantic
497 coast of South America. Conversely, despite having wider coastal plains potentially available
498 for expansion, we expect that populations of *A. schaueriana* occurring north of the NEESA
499 will be threatened by the increased mean temperatures and the decreased precipitation during
500 the El-Niño Southern Oscillation events[8]. The critical temperature threshold is likely to be
501 reached more frequently, intensifying drought events in this region, possibly reducing carbon
502 assimilation and productivity[108] and, in extreme cases, causing biomass loss triggered by
503 cavitation or carbon starvation[109,110]. For the definition of short-term mangrove
504 conservation plans, such as reforestation or restoration of degraded areas on the Atlantic coast
505 of South America, we recommend that populations occurring north and south of the NEESA
506 should warrant attention as distinct conservation management units[111].
507
508 ***3.6 Concluding remarks***
509 Based on the combined analysis of our results, we argue that carbon acquisition in the
510 equatorial region may be limited by the combination of a longer exposure to hypoxia, a higher
511 vapour pressure deficit (VPD) and a higher solar irradiance, especially during the hot and dry

512 season, whereas in the subtropical region, limitations in carbon gain may result from lower
513 solar irradiance levels, lower temperature and shorter photoperiod during winter (Fig 4).
514 These environmental differences between equatorial and subtropical latitudes seem to be
515 shaping gene expression in the field, and remarkably, may have shaped both allele
516 frequencies in genes responding to these variables and morphophysiological traits observed in
517 individuals of *A. schaueriana* (Fig 4). The emergence of this adaptive divergence is facilitated
518 by the limited gene flow identified between populations north and south of the NEESA,
519 possibly driven by the movement of the major ocean currents that are active on the Atlantic
520 coast of South America (Fig 1). Because a similar north-south divergence of neutral
521 molecular markers is also observed for other mangrove and mangrove-associated species on
522 the Atlantic coast of South America[22,23,25], it is also plausible that the environmental
523 drivers of divergence in *A. schaueriana* play a role in the divergence of other species. In
524 addition to revealing that these populations are genetically and functionally distinct
525 units[112], we provide an in-depth empirical evaluation of the intraspecific variation of a
526 long-living non-model tree. We foresee that these results should allow a clearer prediction of
527 how *A. schaueriana* and potentially other mangrove species may respond to the current global
528 climate changes by accounting for phenotypically[7] and genetically[113] informed mangrove
529 distribution modelling.
530

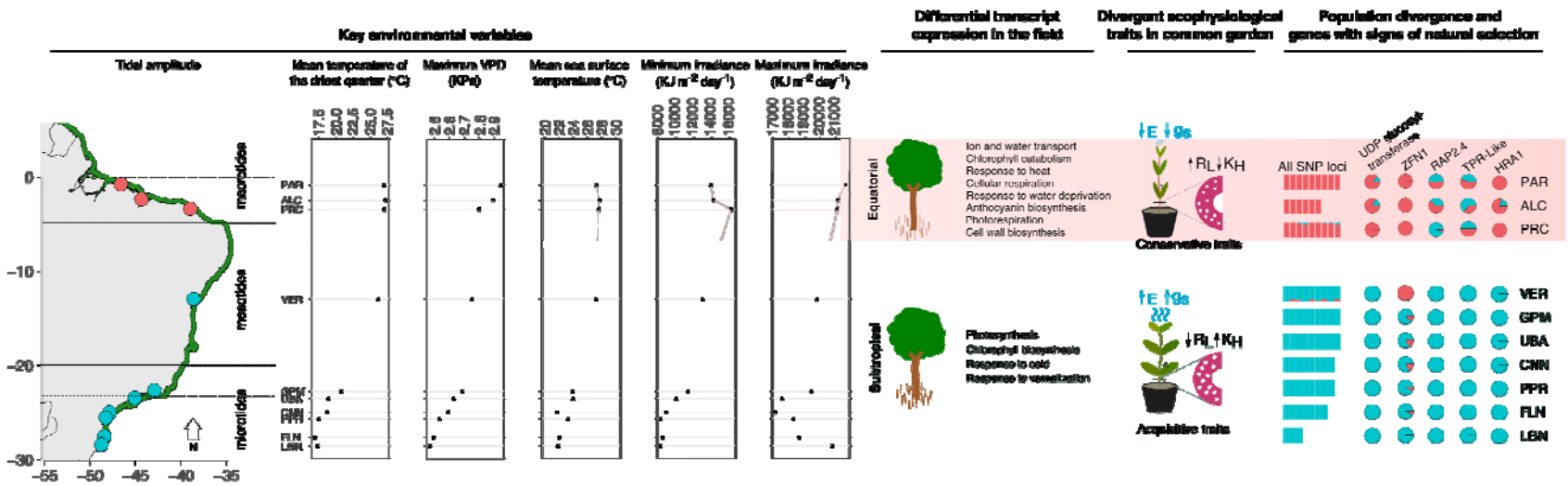

Fig 4. Graphical summary of the integration of ecological and high-throughput genomics data performed in this work.
Key oceanographic and climatic factors differ markedly between equatorial and subtropical latitudinal distribution extremes of the distribution of the neotropical mangrove tree, *Avicennia schaueriana*, possibly shaping the diversity of genotypes and phenotypes of the species. To address this issue, we examined the effects of these contrasting environments on the overall gene expression, its morphophysiological effects in a common garden experiment and its genomic effects through natural selection detection tests based on single nucleotide polymophic (SNP) loci. Plants from equatorial and subtropical latitudes showed key divergences related to the use of water and to the acquisition of carbohydrates both in the field and in common garden conditions. In addition, a north-south genetic divergence was observed in all genotyped SNP loci. We also identified signatures of differential selective pressures on specific loci possibly related to the accumulation of anthocyanin (*UDP-GLUCOSYLTRANSFERASE*), in response to osmotic stress (*RAP2.4* and *ZFN1*), photosynthesis (*TPR*) and hypoxia (*HRA1*). The molecular and ecologic divergences observed through three independent approaches may relate to the environmental factors that strongly differ between contrasting latitudes in which the species are found. These findings highlight the power of using multidisciplinary approaches to the study of adaptation in species with little basic biological information such as tropical trees. VPD: Atmospheric vapour pressure deficit; E: transpiration rate; g_s: stomatal conductance; R_L: xylem vessel lumen resistivity; K_H: xylem vessel conductivity.

546

547 ## 4. Materials and Methods

548 ### *4.1 Propagules sampling sites*

549 Ten mature propagules were collected from ten *A. schaueriana* mother trees belonging
550 to each of two genetically divergent natural populations described in a previous work[22]: one
551 north and one south of the NEESA (Fig 1). Trees were at least 100 m apart from each other at
552 each of the two contrasting sampling points: (1) the southernmost limit of the distribution of
553 American mangroves, in the subtropical region, and (2) one equatorial site in one of the
554 largest macrotidal mangrove forests in the world[29,30], closer to the northernmost limit of
555 the species range (Fig 1). We refer to the former as the 'Subtropical site' and to the latter as
556 the 'Equatorial site' throughout this work. A characterization of each of these sites can be
557 found in Table 1. Further details about these areas can be found in the Supplementary
558 Information file (S1 Method, S1 Fig).

559 To better characterise the climate from the Equatorial and Subtropical sampling sites
560 we have downloaded temperature, relative humidity, rainfall and solar irradiance datasets
561 (2008-2017) from the INMET database (the Meteorological Institute of Brazil) (S1 Fig) and
562 the environmental data from BioClim[31] and MARSPEC[32].

563

564 ### *4.2 Seedlings germination and growth in a common garden experiment*

565 Propagules of *A. schaueriana* sampled from the Equatorial and Subtropical sites
566 germinated on germination trays filled with mangrove soil, under shaded conditions, in open
567 air being irrigated daily with 1:10 (v:v) sea water:tap water solution[33]. After two months,
568 44 similar-sized seedlings from each sampling site — with an average height of 18 cm, most

569 with three leaf pairs and senesced cotyledons — were transplanted to 6 L pots filled with a
570 mixture of topsoil and sand (1:1 ratio). Seedlings were cultivated for seven months under the
571 same environmental conditions in a glasshouse at the University of Campinas, São Paulo,
572 Brazil (22°49' S 47°04' W). Automatic sensors coupled with a data logger (Onset Computer
573 Corp., Bourne, MA, USA) measured the atmospheric humidity and temperature inside the
574 glasshouse every 15 minutes. Seedlings were irrigated by an automated system twice per day
575 (10 a.m. and 5 p.m.), with a 3-minute fresh water spray. Twice a week nutrients were
576 manually added to the soil using 600 mL of 0.4X Hoagland solution with 15.0 g L^{-1} NaCl per
577 pot. All pots were rotated to reduce the effects of eventual environmental heterogeneity. The
578 monitored environmental conditions in the glasshouse differed markedly from both sites of
579 origin (S9 Fig 9). Thus, none of the individuals benefitted from environmental conditions that
580 corresponded to their original sampling site.
581
582 ***4.3 Comparative ecophysiology in a common garden experiment***
583 The light reflectance of stems was measured in 10 plants from each sampling site
584 using a USB4000 spectrophotometer (OceanOptics, Inc., Dunedin, FL, USA) coupled to a
585 deuterium-halogen light source (DH-2000; OceanOptics, Inc., Ostfildern, Germany), using a
586 light emission range from 200-900 nm. To generate a daily curve of photosynthesis, stomatal
587 conductance and transpiration rates, five six-month-old individuals from each sampling site
588 were used for measurements every two or two and a half hours, in two different days, using a
589 Li-Cor 6400 XT (Li-Cor Corp., Lincoln, NE, USA).
590 After harvest, plants that did not present flowers or flower buds were split into three
591 parts: leaves, stems and roots. All plant parts were washed with distilled water, dried for 7
592 days at 70 °C and weighted. A quantitative analysis of key morphological traits was

593 performed using three plants from each site. The individual leaf area, total leaf area and leaf
594 lamina angle were measured per plant through photographs analyses using the ImageJ
595 software[34]. The specific leaf area (SLA, cm^2 leaf area kg^{-1} leaf dry biomass) was also
596 calculated for these same samples. Stems chunks were fixed in FAA (Formaldehyde Alcohol
597 Acetic acid) and stored in 70% alcohol for use in a wood anatomy analysis. Stems were cut
598 into transverse sections with a thickness of 30 μm. Sections were stained with a mixture of
599 1% Astra Blue and 50% alcohol (1:1) followed by 1% Safranin O (diluted in distilled water).
600 Micrographs of the slides were taken using an Olympus BX51 microscope coupled to an
601 Olympus DP71 camera (Olympus Corp., Tokyo, Japan). The following wood traits were
602 quantified using ImageJ[34] and R 4.0: vessel lumen area (A), vessel density in the xylem
603 (number of vessels/xylem area), proportion of solitary vessels (number of solitary
604 vessels/total number of vessels), vessel grouping index (mean number of vessels/vessel
605 grouping), proportion of vessel lumen area in xylem (vessel lumen area/xylem area) and
606 vessel lumen area in sapwood (vessel lumen area/sapwood area). The vessel arithmetic
607 diameter (D), vessel hydraulic conductivity (K_H) and lumen resistivity (R_L) were estimated
608 according to Scholz *et al.*[35].

609 Statistical analyses were performed in R 4.0, with a significance level of 5%, and two-
610 group comparisons were made using the Mann-Whitney-Wilcoxon unpaired test for non-
611 parametric distributions and Student's T-test for parametric distributions. Multiple-group
612 comparisons were conducted using one-way analysis of variance (ANOVA) with post hoc
613 Tukey honest significant difference (HSD) tests.

614

615 ***4.4 Collection of plant material for RNA extraction and RNA-sequencing***

Plant material for RNA-Seq was collected in the "Propagules sampling sites" subsection. Three adult trees were sampled in each sampling site from July-August of 2014, at the end of winter in the Subtropical sampling site and at the beginning of the dry season in the Equatorial sampling site (Table 2, S6 Fig). At each site, we sampled leaves, stems and flowers of trees located at least 100 m apart from each other, from 11:00 am to 4:00 pm, during the low tide, at different altitudes in the intertidal zone (Table 2). Plant material was washed with sodium hypochlorite solution (0.2%), cut with a sterile slide and immediately stored in RNAlater (Ambion Inc., Austin, TX, USA).

Total RNA extraction was performed using a protocol developed by Oliveira et al.[36]. RNA integrity and purity were verified by agarose gel electrophoresis and using a NanoVue spectrophotometer (GE Healthcare Life Sciences, Chalfont, Buckinghamshire, UK). lllumina TruSeq RNA Sample Preparation protocol kits (Illumina Inc., San Diego, CA, USA) were used to construct enriched complimentary DNA (cDNA) libraries. The quality of all libraries was assessed using the Agilent DNA 1000 chip and Agilent 2100 Bioanalyzer (Agilent Technologies, Santa Clara, USA). cDNA libraries concentrations were quantified by qPCR using the Sequencing Library qPCR Quantification kit (Illumina Inc.), followed by sequencing using TruSeq SBS Paired End kits (Illumina Inc.) and a Genome Analyzer IIx sequencer (Illumina Inc.).

4.5 Assembly and characterization of the first reference transcriptome of **A. schaueriana**

Adapter sequences were trimmed and 72 bp paired end reads were filtered by quality (phred score ≥ 20 for at least 70% of read length) using the NGS QC Toolkit 2.3[37]. High-quality reads were used in the subsequent transcriptome assembly in the CLC Genomics

Workbench (https://www.qiagenbioinformatics.com/). We used the default settings and only set the distance between read pairs (300-500 bp), and the k-mer size to 45 bp.

Reads were mapped to the assembled transcripts using bowtie 1[38] in the single-read mode using default parameters. We then removed transcripts that did not present read-mapping support. Functional annotation was performed using the blastx algorithm, available in blast+ v. 2.2.31[39], with an e-value threshold of 1^{-10}. The NCBI RefSeq[40], The Arabidopsis Information Resource (TAIR)[41] and the NCBI non-redundant (nr) databases were used as references. To remove contaminant transcripts, we excluded all transcripts that were exclusively similar to non-plant sequences. Protein family domains were identified using HMMER3[42], which iteratively searched all assembled sequences against the Pfam database. To assign Gene Ontology (GO) terms to transcripts we used the *Arabidopsis thaliana* gene association file from the Gene Ontology Consortium[43] and retrieved the information for transcripts with a similar coding sequence in the genome of *A. thaliana*.

Redundant transcripts were clustered using CD-HIT-EST v. 4.6.1[44], using the local alignment mode, with 95% identity and 70% coverage of the shortest sequence as thresholds. Open reading frames (ORF) in putative protein coding transcripts were identified using the Transdecoder tool (http://transdecoder.sf.net). We reduced redundancy of transcripts in the final assembly by keeping for each CD-HIT-EST cluster either the sequence with the longest ORF or simply the longest sequence, in the absence of sequences containing ORF.

The completeness of the final transcriptome was assessed using BUSCO[45]. Additionally, a reciprocal blastn alignment[39] using an e-value threshold of 10^{-10} and a minimum alignment length of 100 nucleotides with at least 70% identity was used to compare the *A. schaueriana* and other publicly available transcriptomes of congeneric species.

4.6 Comparative transcriptomics using RNA-sequencing data

Tissue-specific count data was obtained from the number of reads uniquely mapped to each transcript of the non-redundant transcriptome using bowtie 1[38]. Count data were normalised using the EdgeR Bioconductor package[46]. Normalised data was used to detect transcripts with significantly different counts between tissue-specific samples of trees at the Equatorial and Subtopical sampling sites, using the exact test for negative binomial distribution, with an adjusted P-value threshold of 0.05. GO term enrichment analyses of the differentially expressed transcripts (DET) were performed using the GOseq package[47], which accounts for length bias. We chose the default Wallenius approximation method and a P-value threshold of 0.05.

Differential expression results were verified using reverse transcription real-time PCR (qRT-PCR) (see S2 Methods).

4.7 Detection of **A. schaueriana** *candidate loci under natural selection using genome-wide SNP data*

We sampled adult plants at 10 locations, spanning most of *A. schaueriana* geographic range, complementing previous population genetic studies[22] by adding the southernmost range limit[28] (Fig 1, S1 Table). We isolated DNA from leaves sampled from 79 trees using the DNeasy Plant Mini Kit (QIAGEN) and NucleoSpin Plant II (Macherey Nagel) following the manufacturer's instructions. DNA quality and quantity were assessed using 1% agarose electrophoresis and the QuantiFluor® dsDNA System in a Quantus™ fluorometer (Promega). Nextera-tagmented, reductively-amplified DNA (nextRAD) libraries were constructed by SNPsaurus (SNPsaurus, LLC), allowing the genotyping of SNP loci across the genome in a consistent manner by using selective primer sequences[48]. Genomic DNA fragmentation and

short adapter ligation were performed with Nextera reagent (Illumina, Inc), followed by amplification, which utilised one of the primers matching the adapter and extending nine arbitrary nucleotides into the genomic DNA. Thus, the resulting amplicons were fixed at the selective end and their lengths depended on the initial Nextera fragmentation, leading to a consistent genotyping of the amplified loci. NextRAD libraries were then sequenced in a HiSeq 2500 (Illumina, Inc.) with 100-bp single-end chemistry following the manufacturer's protocol. Genotyping-by-sequencing used custom scripts (SNPsaurus, LLC), which created a reference catalogue of abundant reads across the combined set of samples. Read mapping to this reference allowed two mismatches. Subsequently, loci presenting sequence variation were filtered for biallelic loci and presence in at least 10% of the total samples. Following assembly, mapping and SNP identification, a second filtering step was performed by allowing no more than 65% of missing data, a Phred score > 30, 8x minimum coverage, only one SNP per loci and a minor allele frequency ≥ 0.05 using vcftools v0.1.12b[49]. To reduce false SNP inclusion rates due to paralogy or low-quality genotype calls, we used a maximum read coverage of 56, which resulted from the product of the average read depth and 1.5 standard deviation.

After excluding plants morphologically identified as *A. schaueriana* with genomic signs of hybridization with *A. germinans*, we described the overall genetic structure in *A. schaueriana* considering both neutral and non-neutral loci in a multivariate model-free method, the discriminant analysis of principal components (DAPC)[50], and in the ADMIXTURE 1.3.0 program[51]. For DAPC analyses, we considered the number of groups varying from 1 to 50 and the Bayesian information criteria for inferring the number of groups (K), in addition to using the optim.a.score function to avoid over-fitting during the discrimination steps. For the ADMIXTURE analyses, we performed three separate runs for K

712 varying between 1 and 15 and using the block-relaxation method for point estimation;
713 computing was terminated when estimates increased by < 0.0001. The K-value that best
714 described our data was determined by cross-validation.

715 To detect signs of natural selection, we used two methods to minimise false-positive
716 results. LOSITAN[52], which uses the FDIST2 method[53], assuming an infinite allele model
717 of mutation, using a confidence interval of 0.99, a false-discovery rate (FDR) of 0.1, the
718 neutral mean FST and forcing the mean FST options, and pcadapt 3.0.4[54], which
719 simultaneously identifies the population structure and the loci excessively related to this
720 structure, using an FDR threshold of 0.1.

721 The sequences in which loci with putative evidence of selection were identified
722 simultaneously by pcadapt and by five independent runs of LOSITAN were searched within
723 expressed regions of the reference transcriptome. A reciprocal alignment between the short
724 sequences obtained through nextRAD (75 bp) and the longer expressed sequences assembled
725 from RNA-Seq data (≈ 300-11600 bp) was performed. The alignment was conducted using
726 the blastn algorithm from the blast+ software v. 2.2.31[39], with a threshold of at least 50
727 aligned nucleotides, a maximum of one mismatch and no gaps.

728 ## 5. Acknowledgements

729 We thank Professors Dr. Michel A. G. Vincentz and Dr. Juliana L. S. Mayer for
730 advising and making available their laboratory for our training and performing of,
731 respectively, RNA extraction procedures and slides preparation used in the analyses of wood
732 anatomy. We acknowledge Ilmarina C. de Menezes and Stephanie K. Bajay for assistance in
733 the field. We thank Stephanie K. Bajay for also giving assistance in the germination of the
734 propagules used in the common garden experiment. And we thank Greg Mellers and

Alessandro A. Pereira for critically reading the manuscript. M.V.C and G.M.M. received fellowships from the São Paulo Research Foundation (FAPESP 2013/26793-7, 2013/08086-1 and 2014/22821-9). M.V.C. received fellowship from the Coordination for the Improvement of Higher Education Personnel (CAPES 8084/2015-07, Biocomputational Biology Program). G.M.M. received grant from the Brazilian National Council for Scientific and Technological Development (CNPq 448286/2014-9). A.P.S. was supported by grant from CAPES (Biocomputational Biology Program), and a received a research fellowship from CNPq (309661/2014-5).

6. References

1. Hereford J. A Quantitative Survey of Local Adaptation and Fitness Trade□Offs. Am Nat. 2009;173: 579–588. doi:10.1086/597611
2. Kawecki TJ, Ebert D. Conceptual issues in local adaptation. Ecol Lett. 2004;7: 1225–1241. doi:10.1111/j.1461-0248.2004.00684.x
3. Leimu R, Fischer M. A meta-analysis of local adaptation in plants. PLoS One. 2008;3: 1–8. doi:10.1371/journal.pone.0004010
4. Albert CH, Grassein F, Schurr FM, Vieilledent G, Violle C. When and how should intraspecific variability be considered in trait-based plant ecology? Perspect Plant Ecol Evol Syst. 2011;13: 217–225. doi:10.1016/j.ppees.2011.04.003
5. Savolainen O, Lascoux M, Merilä J. Ecological genomics of local adaptation. Nat Rev Genet. Nature Publishing Group; 2013;14: 807–20. doi:10.1038/nrg3522
6. Barrett RDH, Hoekstra HE. Molecular spandrels: tests of adaptation at the genetic level. Nat Rev Genet. Nature Publishing Group; 2011;12: 767–780. doi:10.1038/nrg3015

7. Moran E V., Hartig F, Bell DM. Intraspecific trait variation across scales: Implications for understanding global change responses. Glob Chang Biol. 2016;22: 137–150. doi:10.1111/gcb.13000

8. Pachauri RK, Meyer LA, editors. Climate Change 2014: Synthesis Report. Contribution of Working Groups I, II and III to the Fifth Assessment Report of the Intergovernmental Panel on Climate Change. IPCC. Geneva, Switzerland: IPCC; 2014.

9. Loarie SR, Duffy PB, Hamilton H, Asner GP, Field CB, Ackerly DD. The velocity of climate change. Nature. Nature Publishing Group; 2009;462: 1052–1055. doi:10.1038/nature08649

10. Osland MJ, Feher LC, Griffith KT, Cavanaugh KC, Enwright NM, Day RH, et al. Climatic controls on the global distribution, abundance, and species richness of mangrove forests. Ecol Monogr. 2017;87: 341–359. doi:10.1002/ecm.1248

11. Lovelock CE, Cahoon DR, Friess DA, Guntenspergen GR, Krauss KW, Reef R, et al. The vulnerability of Indo-Pacific mangrove forests to sea-level rise. Nature. 2015;526: 559–563. doi:10.1038/nature15538

12. Nascimento Jr. WR, Souza-Filho PWM, Proisy C, Lucas RM, Rosenqvist A. Mapping changes in the largest continuous Amazonian mangrove belt using object-based classification of multisensor satellite imagery. Estuar Coast Shelf Sci. 2013;117: 83–93. doi:10.1016/j.ecss.2012.10.005

13. Shearman P, Bryan J, Walsh JP. Trends in Deltaic Change over Three Decades in the Asia-Pacific Region. J Coast Res. 2013;29: 1169–1183. doi:10.2112/JCOASTRES-D-12-00120.1

14. Cavanaugh KC, Kellner JR, Forde AJ, Gruner DS, Parker JD, Rodriguez W, et al. Poleward expansion of mangroves is a threshold response to decreased frequency of

extreme cold events. Proc Natl Acad Sci U S A. 2014;111: 723–7. doi:10.1073/pnas.1315800111

15. Saintilan N, Wilson NC, Rogers K, Rajkaran A, Krauss KW. Mangrove expansion and salt marsh decline at mangrove poleward limits. Glob Chang Biol. 2014;20: 147–157. doi:10.1111/gcb.12341

16. Duke N, Kovacs J, Griffiths A, Preece L, J. E. Hill D, Van Oosterzee P, et al. Large-scale dieback of mangroves in Australia. Marine and Freshwater Research. 2017. doi:10.1071/MF16322

17. Eslami-Andargoli L, Dale P, Sipe N, Chaseling J. Mangrove expansion and rainfall patterns in Moreton Bay, Southeast Queensland, Australia. Estuar Coast Shelf Sci. Elsevier Ltd; 2009;85: 292–298. doi:10.1016/j.ecss.2009.08.011

18. Alongi DM. The Impact of Climate Change on Mangrove Forests. Curr clim Chang Rep. 2015;4: 516. doi:10.1007/s40641-015-0002-x

19. McKee KL, Cahoon DR, Feller IC. Caribbean mangroves adjust to rising sea level through biotic controls on change in soil elevation. Glob Ecol Biogeogr. 2007;16: 545–556. doi:10.1111/j.1466-8238.2007.00317.x

20. López-Medellín X, Ezcurra E, González-Abraham C, Hak J, Santiago LS, Sickman JO. Oceanographic anomalies and sea-level rise drive mangroves inland in the Pacific coast of Mexico. J Veg Sci. 2011;22: 143–151. doi:10.1111/j.1654-1103.2010.01232.x

21. Doyle TW, Krauss KW, Conner WH, From AS. Forest Ecology and Management Predicting the retreat and migration of tidal forests along the northern Gulf of Mexico under sea-level rise. For Ecol Manage. 2010;259: 770–777. doi:10.1016/j.foreco.2009.10.023

22. Mori GM, Zucchi MI, Souza AP. Multiple-Geographic-Scale Genetic Structure of Two

Mangrove Tree Species: The Roles of Mating System, Hybridization, Limited Dispersal and Extrinsic Factors. PLoS One. 2015;10: e0118710. doi:10.1371/journal.pone.0118710

23. Francisco PM, Mori GM, Alves FM, Tambarussi E, Souza AP De. Population genetic structure, introgression, and hybridization in the genus Rhizophora along the Brazilian coast. Ecol Evol. 2018; 1–14. doi:10.1002/ece3.3900

24. Pil MW, Boeger MRT, Muschner VC, Pie MR, Ostrensky A, Boeger W a. Postglacial north-south expansion of populations of Rhizophora mangle (Rhizophoraceae) along the Brazilian coast revealed by microsatellite analysis. Am J Bot. 2011;98: 1031–1039. doi:10.3732/ajb.1000392

25. Takayama K, Tateishi Y, Murata J, Kajita T. Gene flow and population subdivision in a pantropical plant with sea-drifted seeds Hibiscus tiliaceus and its allied species: Evidence from microsatellite analyses. Mol Ecol. 2008;17: 2730–2742. doi:10.1111/j.1365-294X.2008.03799.x

26. Savolainen O, Pyhäjärvi T, Knürr T. Gene Flow and Local Adaptation in Trees. Annu Rev Ecol Evol Syst. 2007;38: 595–619. doi:10.1146/annurev.ecolsys.38.091206.095646

27. Andrews KR, Good JM, Miller MR, Luikart G, Hohenlohe PA. Harnessing the power of RADseq for ecological and evolutionary genomics. Nat Rev Genet. Nature Publishing Group; 2016;17: 81–92. doi:10.1038/nrg.2015.28

28. Soares MLG, Estrada GCD, Fernandez V, Tognella MMP. Southern limit of the Western South Atlantic mangroves: Assessment of the potential effects of global warming from a biogeographical perspective. Estuar Coast Shelf Sci. Elsevier Ltd; 2012;101: 44–53. doi:10.1016/j.ecss.2012.02.018

29. Souza-Filho PWM, Cohen MCL, Lara RJ, Lessa GC, Koch B, Behling H. Holocene Coastal Evolution and Facies Model of the Bragança Macrotidal Flat on the Amazon Mangrove Coast, Northern Brazil. J Coast Res. 2006; 306–310.

30. Kjerfve B, Perillo GME, Gardner LR, Rine JM, Dias GTM, Mochel FR. Chapter Twenty Morphodynamics of muddy environments along the Atlantic coasts of North and South America. Proc Mar Sci. Elsevier; 2002;4: 479–532. doi:10.1016/S1568-2692(02)80094-8

31. Hijmans RJ, Cameron SE, Parra JL, Jones PG, Jarvis A. Very high resolution interpolated climate surfaces for global land areas. Int J Climatol. 2005;25: 1965–1978. doi:10.1002/joc.1276

32. Sbrocco EJ, Barber PH. MARSPEC: ocean climate layers for marine spatial ecology. Ecology. 2013;94: 979–979. doi:10.1890/12-1358.1

33. Reef R, Winter K, Morales J, Adame MF, Reef DL, Lovelock CE. The effect of atmospheric carbon dioxide concentrations on the performance of the mangrove Avicennia germinans over a range of salinities. Physiol Plant. 2014;154. doi:10.1111/ppl.12289

34. Schneider CA, Rasband WS, Eliceiri KW. NIH Image to ImageJ□: 25 years of image analysis. Nat Methods. Nature Publishing Group; 2012;9: 671–675. doi:10.1038/nmeth.2089

35. Scholz A, Klepsch M, Karimi Z, Jansen S. How to quantify conduits in wood? Front Plant Sci. 2013;4: 1–11. doi:10.3389/fpls.2013.00056

36. Oliveira RR, Viana AJC, Reátegui ACE, Vincentz MGA. An efficient method for simultaneous extraction of high-quality RNA and DNA from various plant tissues. Genet Mol Res. 2015;14: 18828–18838. doi:10.4238/2015.December.28.32

854 37. Patel RK, Jain M. NGS QC toolkit: A toolkit for quality control of next generation
855 sequencing data. PLoS One. 2012;7. doi:10.1371/journal.pone.0030619
856 38. Langmead B, Trapnell C, Pop M, Salzberg S. Ultrafast and memory-efficient
857 alignment of short DNA sequences to the human genome. Genome Biol. 2009;10: R25.
858 doi:10.1186/gb-2009-10-3-r25
859 39. Camacho C, Coulouris G, Avagyan V, Ma N, Papadopoulos J, Bealer K, et al.
860 BLAST+: architecture and applications. BMC Bioinformatics. 2009;10: 421.
861 doi:10.1186/1471-2105-10-421
862 40. O'Leary NA, Wright MW, Brister JR, Ciufo S, Haddad D, McVeigh R, et al.
863 Reference sequence (RefSeq) database at NCBI: Current status, taxonomic expansion,
864 and functional annotation. Nucleic Acids Res. 2016;44: D733–D745.
865 doi:10.1093/nar/gkv1189
866 41. Berardini TZ, Reiser L, Li D, Mezheritsky Y, Muller R, Strait E, et al. The Arabidopsis
867 Information Resource□: Making and Mining the " Gold Standard " Annotated
868 Reference Plant Genome. Genesis. 2015;53: 474–485. doi:10.1002/dvg.22877
869 42. Finn RD, Bateman A, Clements J, Coggill P, Eberhardt RY, Eddy SR, et al. Pfam: The
870 protein families database. Nucleic Acids Res. 2014;42: 222–230.
871 doi:10.1093/nar/gkt1223
872 43. Blake JA, Christie KR, Dolan ME, Drabkin HJ, Hill DP, Ni L, et al. Gene ontology
873 consortium: Going forward. Nucleic Acids Res. 2015;43: D1049–D1056.
874 doi:10.1093/nar/gku1179
875 44. Li W, Godzik A. Cd-hit: A fast program for clustering and comparing large sets of
876 protein or nucleotide sequences. Bioinformatics. 2006;22: 1658–1659.
877 doi:10.1093/bioinformatics/btl158

878 45. Simão FA, Waterhouse RM, Ioannidis P, Kriventseva E V., Zdobnov EM. BUSCO:
879 Assessing genome assembly and annotation completeness with single-copy orthologs.
880 Bioinformatics. 2015;31: 3210–3212. doi:10.1093/bioinformatics/btv351
881 46. Robinson MD, McCarthy DJ, Smyth GK. edgeR: a Bioconductor package for
882 differential expression analysis of digital gene expression data. Bioinformatics.
883 2010;26: 139–140. doi:10.1093/bioinformatics/btp616
884 47. Young MD, Wakefield MJ, Smyth GK, Oshlack A. Gene ontology analysis for RNA-
885 seq: accounting for selection bias. Genome Biol. 2010;11. doi:10.1186/gb-2010-11-2-
886 r14
887 48. Russello MA, Waterhouse MD, Etter PD, Johnson EA. From promise to practice:
888 pairing non-invasive sampling with genomics in conservation. PeerJ. 2015;3: e1106.
889 doi:10.7717/peerj.1106
890 49. Danecek P, Auton A, Abecasis G, Albers CA, Banks E, DePristo MA, et al. The
891 variant call format and VCFtools. Bioinformatics. 2011;27: 2156–2158.
892 doi:10.1093/bioinformatics/btr330
893 50. Jombart T, Devillard S, Balloux F. Discriminant analysis of principal components: a
894 new method for the analysis of genetically structured populations. BMC Genet.
895 BioMed Central Ltd; 2010;11: 94. doi:10.1186/1471-2156-11-94
896 51. Alexander DH, Novembre J, Lange K. Fast model-based estimation of ancestry in
897 unrelated individuals. Genome Res. 2009;19: 1655–1664. doi:10.1101/gr.094052.109
898 52. Antao T, Lopes A, Lopes RJ, Beja-Pereira A, Luikart G. LOSITAN: A workbench to
899 detect molecular adaptation based on a F st -outlier method. BMC Bioinformatics.
900 2008;9: 1–5. doi:10.1186/1471-2105-9-323
901 53. Beaumont MA, Nichols RA. Evaluating Loci for Use in the Genetic Analysis of

902 Population Structure. Proc R Soc B Biol Sci. 1996;263: 1619–1626.
903 doi:10.1098/rspb.1996.0237

904 54. Luu K, Bazin E, Blum MGB. pcadapt: An R package to perform genome scans for
905 selection based on principal component analysis. Mol Ecol Resour. 2016;33: 67–77.
906 doi:10.1111/1755-0998.12592

907 55. Wang Z, Gerstein M, Snyder M. RNA-Seq: a revolutionary tool for transcriptomics.
908 Nat Rev Genet. 2009;10: 57–63.

909 56. Huang J, Lu X, Zhang W, Huang R, Chen S, Zheng Y. Transcriptome Sequencing and
910 Analysis of Leaf Tissue of Avicennia marina Using the Illumina Platform. PLoS One.
911 2014;9: e108785. doi:10.1371/journal.pone.0108785

912 57. Lyu H, Li X, Guo Z, He Z, Shi S. De novo assembly and annotation of the Avicennia
913 officinalis L. transcriptome. Mar Genomics. Elsevier B.V.; 2017; 2–5.
914 doi:10.1016/j.margen.2017.07.002

915 58. Krishnamurthy P, Mohanty B, Wijaya E, Lee D, Lim T, Lin Q, et al. Transcriptomics
916 analysis of salt stress tolerance in the roots of the mangrove Avicennia officinalis. Nat
917 Sci Reports. 2017;7: 1–19. doi:10.1038/s41598-017-10730-2

918 59. Park S-Y, Yu J-W, Park J-S, Li J, Yoo S-C, Lee N-Y, et al. The Senescence-Induced
919 Staygreen Protein Regulates Chlorophyll Degradation. Plant Cell. 2007;19: 1649–
920 1664. doi:10.1105/tpc.106.044891

921 60. Myouga F, Hosoda C, Umezawa T, Iizumi H, Kuromori T, Motohashi R, et al. A
922 Heterocomplex of Iron Superoxide Dismutases Defends Chloroplast Nucleoids against
923 Oxidative Stress and Is Essential for Chloroplast Development in Arabidopsis. Plant
924 Cell Online. 2008;20: 3148–3162. doi:10.1105/tpc.108.061341

925 61. Wang S, Bai G, Wang S, Yang L, Yang F, Wang Y. Chloroplast RNA-Binding Protein

RBD1 Promotes Chilling Tolerance through 23S rRNA Processing in Arabidopsis. PLoS Genet. 2016;12: 1–21. doi:10.1371/journal.pgen.1006027

62. Goulas E, Schubert M, Kieselbach T, Kleczkowski LA, Gardestro P, Schro W. The chloroplast lumen and stromal proteomes of Arabidopsis thaliana show differential sensitivity to short- and long-term exposure to low temperature. Plant J. 2006;47: 720–734. doi:10.1111/j.1365-313X.2006.02821.x

63. Kim YO, Kim JS, Kang H. Cold-inducible zinc finger-containing glycine-rich RNA-binding protein contributes to the enhancement of freezing tolerance in Arabidopsis thaliana. Plant J. 2005;42: 890–900. doi:10.1111/j.1365-313X.2005.02420.x

64. Hartung F, Suer S, Puchta H. Two closely related RecQ helicases have antagonistic roles in homologous recombination and DNA repair in Arabidopsis thaliana. Proc Natl Acad Sci. 2007;104: 18836–18841. doi:10.1073/pnas.0705998104

65. Michaels SD, Ditta G, Gustafson-Brown C, Pelaz S, Yanofsky M, Amasino RM. AGL24 acts as a promoter of flowering in Arabidopsis and is positively regulated by vernalization. Plant J. 2003;33: 867–874. doi:10.1046/j.1365-313X.2003.01671.x

66. Jung YJ, Melencion SMB, Lee ES, Park JH, Alinapon CV, Oh HT, et al. Universal Stress Protein Exhibits a Redox-Dependent Chaperone Function in Arabidopsis and Enhances Plant Tolerance to Heat Shock and Oxidative Stress. Front Plant Sci. 2015;6: 1–11. doi:10.3389/fpls.2015.01141

67. Ogawa T, Pan L, Kawai-Yamada M, Yu L-H, Yamamura S, Koyama T, et al. Functional Analysis of Arabidopsis Ethylene-Responsive Element Binding Protein Conferring Resistance to Bax. Plant Physiol. 2005;138: 1436–1445. doi:10.1104/pp.105.063586.1436

68. Lin RC, Park HJ, Wang HY. Role of Arabidopsis RAP2.4 in regulating light- and

ethylene-mediated developmental processes and drought stress tolerance. Mol Plant. The Authors 2007. All rights reserved.; 2008;1: 42–57. doi:10.1093/mp/ssm004

69. Rae L, Lao NT, Kavanagh TA. Regulation of multiple aquaporin genes in Arabidopsis by a pair of recently duplicated DREB transcription factors. Planta. 2011;234: 429–444. doi:10.1007/s00425-011-1414-z

70. Alexandersson E, Fraysse L, Sjövall-Larsen S, Gustavsson S, Fellert M, Karlsson M, et al. Whole gene family expression and drought stress regulation of aquaporins. Plant Mol Biol. 2005;59: 469–484. doi:10.1007/s11103-005-0352-1

71. Nishizawa A, Yabuta Y, Shigeoka S. Galactinol and Raffinose Constitute a Novel Function to Protect Plants from Oxidative Damage. Plant Physiol. 2008;147: 1251–1263. doi:10.1104/pp.108.122465

72. Zhang A, Ren H-M, Tan Y-Q, Qi G-N, Yao F-Y, Wu G-L, et al. S-Type Anion Channels SLAC1 and SLAH3 Function as Essential Negative Regulators of Inward K^+ Channels and Stomatal Opening in Arabidopsis. Plant Cell. 2016;28: 949–965. doi:10.1105/tpc.15.01050

73. Liepman AH, Olsen LJ. Alanine aminotransferase homologs catalyze the glutamate:glyoxylate aminotransferase reaction in peroxisomes of Arabidopsis. Plant Physiol. 2003;131: 215–27. doi:10.1104/pp.011460

74. Wolf JBW, Lindell J, Backstrom N. Speciation genetics: current status and evolving approaches. Philos Trans R Soc B Biol Sci. 2010;365: 1717–1733. doi:10.1098/rstb.2010.0023

75. Ahrens CW, Rymer PD, Stow A, Bragg J, Dillon S, Umbers KDL, et al. The search for loci under selection: trends, biases and progress. Mol Ecol. 2018; doi:doi.org/10.1111/mec.14549

974 76. Sakamoto H, Araki T, Meshi T, Iwabuchi M. Expression of a subset of the Arabidopsis
975 Cys2/His2-type zinc-finger protein gene family under water stress. Gene. 2000;248:
976 23–32. doi:10.1016/S0378-1119(00)00133-5
977 77. Giuntoli B, Lee SC, Licausi F, Kosmacz M, Oosumi T, van Dongen JT, et al. A
978 Trihelix DNA Binding Protein Counterbalances Hypoxia-Responsive Transcriptional
979 Activation in Arabidopsis. PLoS Biol. 2014;12. doi:10.1371/journal.pbio.1001950
980 78. Tohge T, Nishiyama Y, Hirai MY, Yano M, Nakajima JI, Awazuhara M, et al.
981 Functional genomics by integrated analysis of metabolome and transcriptome of
982 Arabidopsis plants over-expressing an MYB transcription factor. Plant J. 2005;42:
983 218–235. doi:10.1111/j.1365-313X.2005.02371.x
984 79. Bohne A V., Schwenkert S, Grimm B, Nickelsen J. Roles of Tetratricopeptide Repeat
985 Proteins in Biogenesis of the Photosynthetic Apparatus [Internet]. International Review
986 of Cell and Molecular Biology. Elsevier Inc.; 2016. doi:10.1016/bs.ircmb.2016.01.005
987 80. Reef R, Lovelock CE. Regulation of water balance in Mangroves. Ann Bot. 2015;115:
988 385–395. doi:10.1093/aob/mcu174
989 81. Steyn WJ, Wand SJE, Holcroft DM, Jacobs G. Anthocyanins in vegetative tissues: a
990 proposed unified function in photoprotection. New Phytol. 2002;155: 349–361.
991 doi:10.1046/j.1469-8137.2002.00482.x
992 82. Menezes MPM de, Berger U, Mehlig U. Mangrove vegetation in Amazonia: a review
993 of studies from the coast of Pará and Maranhão States, north Brazil. Acta Amaz.
994 2008;38: 403–420. doi:10.1590/S0044-59672008000300004
995 83. De Alvarenga AMSB, Botosso PC, Soffiatti P. Stem growth and phenology of three
996 subtropical mangrove tree species. Brazilian J Bot. 2017; doi:10.1007/s40415-017-
997 0397-9

998 84. Kazan K, Lyons R. The link between flowering time and stress tolerance. J Exp Bot.
999 2016;67: 47–60. doi:10.1093/jxb/erv441
1000 85. Stuart SA, Choat B, Martin KC, Holbrook NM, Ball MC. The role of freezing in
1001 setting the latitudinal limits of mangrove forests. New Phytol. 2006;173: 576–583.
1002 doi:10.1111/j.1469-8137.2006.01938.x
1003 86. Carlson JE, Holsinger KE, Prunier R. Plant responses to climate in the cape floristic
1004 region of South Africa: Evidence for adaptive differentiation in the proteaceae.
1005 Evolution (N Y). 2011;65: 108–124. doi:10.1111/j.1558-5646.2010.01131.x
1006 87. Saenger P, Snedaker SC. Pantropical trends in mangrove above-ground biomass and
1007 annual litterfall. Oecologia. 1993;96: 293–299. doi:10.1007/BF00317496
1008 88. Krishnamurthy P, Jyothi-Prakash PA, Qin L, He J, Lin Q, Loh CS, et al. Role of root
1009 hydrophobic barriers in salt exclusion of a mangrove plant Avicennia officinalis. Plant,
1010 Cell Environ. 2014;37: 1656–1671. doi:10.1111/pce.12272
1011 89. Maurel C, Verdoucq L, Luu D-T, Santoni V. Plant Aquaporins: Membrane Channels
1012 with Multiple Integrated Functions. Annu Rev Plant Biol. 2008;59: 595–624.
1013 doi:10.1146/annurev.arplant.59.032607.092734
1014 90. Gall H Le, Philippe F, Domon J-M, Gillet F, Pelloux J, Rayon C. Cell Wall
1015 Metabolism in Response to Abiotic Stress. Plants. 2015;4: 112–166.
1016 doi:10.3390/plants4010112
1017 91. Pecot SD, Horsley SB, Battaglia MA, Mitchell RJ. The influence of canopy, sky
1018 condition, and solar angle on light quality in a longleaf pine woodland. Can J For Res.
1019 2005;35: 1356–1366. doi:10.1139/x05-069
1020 92. Kimura M, Yamamoto YY, Seki M, Sakurai T, Sato M, Abe T, et al. Identification of
1021 Arabidopsis Genes Regulated by High Light – Stress Using cDNA Microarray.

1022 Photochem Photobiol. 2003;77: 226–233. doi:https://doi.org/10.1562/0031-8655

1023 93. Murchie EH, Hubbart S, Peng S, Horton P. Acclimation of photosynthesis to high
1024 irradiance in rice: Gene expression and interactions with leaf development. J Exp Bot.
1025 2005;56: 449–460. doi:10.1093/jxb/eri100

1026 94. Wang D, Pan Y, Zhao X, Zhu L, Fu B, Li Z. Genome-wide temporal-spatial gene
1027 expression profiling of drought responsiveness in rice. BMC Genomics. 2011;12.
1028 doi:10.1186/1471-2164-12-149

1029 95. Moumeni A, Satoh K, Kondoh H, Asano T, Hosaka A, Venuprasad R, et al.
1030 Comparative analysis of root transcriptome profiles of two pairs of drought-tolerant
1031 and susceptible rice near-isogenic lines under different drought stress. BMC Plant Biol.
1032 2011;11. doi:10.1186/1471-2229-11-174

1033 96. Bray EA. Genes commonly regulated by water-deficit stress in Arabidopsis thaliana. J
1034 Exp Bot. 2004;55: 2331–2341. doi:10.1093/jxb/erh270

1035 97. Zhang C, Zhang L, Zhang S, Zhu S, Wu P, Chen Y, et al. Global analysis of gene
1036 expression profiles in physic nut (Jatropha curcas L.) seedlings exposed to drought
1037 stress. BMC Plant Biol. 2015;15: 1–14. doi:10.1186/s12870-014-0397-x

1038 98. Hasanuzzaman M, Nahar K, Alam MM, Roychowdhury R, Fujita M. Physiological,
1039 biochemical, and molecular mechanisms of heat stress tolerance in plants. Int J Mol
1040 Sci. 2013;14: 9643–9684. doi:10.3390/ijms14059643

1041 99. Han F, Chen H, Li XJ, Yang MF, Liu GS, Shen SH. A comparative proteomic analysis
1042 of rice seedlings under various high-temperature stresses. Biochim Biophys Acta.
1043 Elsevier B.V.; 2009;1794: 1625–1634. doi:10.1016/j.bbapap.2009.07.013

1044 100. Wong CE, Li Y, Labbe A, Guevara D, Nuin P, Whitty B, et al. Transcriptional
1045 profiling implicates novel interactions between abiotic stress and hormonal responses

in Thellungiella, a close relative of Arabidopsis. Plant Physiol. 2006;140: 1437–1450. doi:10.1104/pp.105.070508

101. Munné-Bosch S, Alegre L. Die and let live: Leaf senescence contributes to plant survival under drought stress. Funct Plant Biol. 2004;31: 203–216. doi:10.1071/FP03236

102. Millar AH, Whelan J, Soole KL, Day DA. Organization and Regulation of Mitochondrial Respiration in Plants. Annu Rev Plant Biol. 2011;62: 79–104. doi:10.1146/annurev-arplant-042110-103857

103. Raghavendra AS, Padmasree K. Beneficial interactions of mitochondrial metabolism with photosynthetic carbon assimilation. Trends Plant Sci. 2003;8: 546–553. doi:10.1016/j.tplants.2003.09.015

104. Atkin OK, Macherel D. The crucial role of plant mitochondria in orchestrating drought tolerance. Ann Bot. 2009;103: 581–597. doi:10.1093/aob/mcn094

105. Schaeffer-Novelli Y, Cintrón-Molero G, Adaime RR, de Camargo TM. Variability of mangrove ecosystems along the Brazilian coast. Estuaries. 1990;13: 204–218. doi:10.1007/BF02689854

106. Godoy MDP, De Lacerda LD. Mangroves Response to Climate Change: A Review of Recent Findings on Mangrove Extension and Distribution. Ann Brazilian Acad Sci. 2015;87: 651–667. doi:10.1590/0001-3765201520150055

107. Ellison JC. Vulnerability assessment of mangroves to climate change and sea-level rise impacts. Wetl Ecol Manag. 2015;23: 115–137. doi:10.1007/s11273-014-9397-8

108. Saenger P, Moverly J. Vegetative phenology along the Queensland coastline. Proc Ecol Soc Aust. 1985;13: 257–265.

109. Doughty CE, Metcalfe DB, Girardin CAJ, Amézquita FF, Cabrera DG, Huasco WH, et

al. Drought impact on forest carbon dynamics and fluxes in Amazonia. Nature. 2015;519: 78–82. doi:10.1038/nature14213

110. Rowland L, da Costa ACL, Galbraith DR, Oliveira RS, Binks OJ, Oliveira AAR, et al. Death from drought in tropical forests is triggered by hydraulics not carbon starvation. Nature. 2015;528: 119–122. doi:https://doi.org/10.1038/nature15539

111. Moritz C. Defining "Evolutionarily Significant Units" for conservation. Trends Ecol Evol. 1994;9: 373–375. doi:10.1016/0169-5347(94)90057-4

112. Wee AKS, Mori GM, Lira-Medeiros CF, Núñez-Farfán J, Takayama K, Faulks L, et al. The integration and application of genomic information in mangrove conservation. Conserv Biol. 2018; 1–40. doi:10.1111/cobi.13140

113. Ikeda DH, Max TL, Allan GJ, Lau MK, Shuster SM, Whitham TG. Genetically informed ecological niche models improve climate change predictions. Glob Chang Biol. 2017;23: 164–176. doi:10.1111/gcb.13470

114. Alvares CA, Stape JL, Sentelhas PC, Gonçalves JL de M, Sparovek G. Köppen's climate classification map for Brazil. Meteorol Zeitschrift. 2013;22: 711–728. doi:10.1127/0941-2948/2013/0507

115. Forsythe WC, Rykiel EJ, Stahl RS, Wu H i., Schoolfield RM. A model comparison for daylength as a function of latitude and day of year. Ecol Modell. 1995;80: 87–95. doi:10.1016/0304-3800(94)00034-F

116. McRae GJ. A Simple Procedure for Calculating Atmospheric Water Vapor Concentration. J Air Pollut Control Assoc. 1980;30: 394–394. doi:10.1080/00022470.1980.10464362

6. Supporting information captions

S1 Fig. Climate characterisation of Equatorial and Subtropical sampling sites. Points represent the monthly means of climate variables (2008-2017). Red line: Equatorial site (Tracuateua automatic station); blue line: Subtropical site (Santa Marta automatic station). Source: Brazilian National Institute of Meteorology (INMET). (A) Average temperature; (B) average maximum temperature; (C) average minimum temperature; (D) average solar irradiance; (E) total precipitation; (F) average air humidity; (G) average air vapour pressure deficit (VPD), estimated according to McRae(McRae, 1980).

S2 Fig. Daily curves of gas exchange in leaves of seven-months-old *Avicennia schaueriana* seedlings grown in a common-garden. Points represent the means ± standard error bars. Stars (*) represent rejection of the null hypothesis of the absence of a difference based on the unpaired Student's t-test at a significance threshold of 0.05 (n = 10 plants per group). Red line: equatorial origin; blue line: Subtropical origin. (A) Transpiration rate; (B) stomatal conductance; (C) rate of net CO_2 assimilation.

S3 Fig. *Avicennia schaueriana* from Equatorial and Subtropical sites grown in common-garden. (A) Geographical distribution of the species (green shaded zone) and location of the Equatorial (red dot) and the Subtropical (blue dot) sampling sites of propagules used in the experiment conducted in a green house (black square); (B) propagules germinating in trays filled with mangrove soil; (C-D) seedlings from the Equatorial and from the Subtropical sampling sites on the 80th day of the experiment; (E-F) seedlings from the Equatorial and Subtropical sampling sites on the 225th day of the experiment; (G) seven-months-old

Avicennia schaueriana from the Equatorial sampling site presenting flower buds and flowers; (H-I) micrographs of stem transverse sections from pith to the outermost growth section of one representative seedling from the Equatorial and Subtropical sampling sites (magnification = 10x); stem sections were stained with Astra Blue and Safranin O; V: xylem vessels; Ph: phloem; CCC: vascular cambium.

S4 Fig. Sampling of *Avicennia schaueriana* plant material used for RNA-Sequencing. (A) Geographical distribution of the species (green zone) and locations of the Equatorial (red dot) and Subtropical (blue dot) sampling sites; (B) sampling in the native environment (top) and plant organs used for RNA extraction and sequencing (bottom).

S5 Fig. Characterisation of the *de novo* assembly of the *Avicennia schaueriana* reference transcriptome. (A) Histogram of the length of putative protein-coding and putative non-coding transcripts; (B) classification of all predicted open reading frames (ORF) in the reference transcriptome: complete, partial 3' (missing stop codon), partial 5' (missing start codon), internal (missing both start and stop codons); (C) annotation of transcripts via blastx using The *Arabidopsis* Information Resource (TAIR) protein database and The National Center for Biotechnology Information (NCBI) RefSeq Plant protein database; (D) blastx top-hit species distribution of transcripts annotations using NCBI RefSeq Plant protein database as reference.

S6 Fig. Detection of differentially expressed transcripts (DET) and Gene Ontology (GO) enrichment analysis. (A-C) Two-dimensional scatterplot of distances among transcript expression profiles in leaf, stem and flower samples (left to right) of *Avicennia schaueriana* trees under field conditions; points represent individual samples, and distances are

1142 approximately the log2-transformed fold changes between samples; red points represent
1143 samples from the Equatorial site and blue points represent samples from the Subtropical site.
1144 (D-F) MA-plots of transcript expression in leaves, stems and flowers; red points represent
1145 DET overexpressed in Equatorial samples; blue points represent DET overexpressed in
1146 Subtropical samples; black points represent non-differentially expressed transcripts; grey
1147 horizontal lines represent ± 1 log fold-change threshold. (G-H) Proportion of DET used in the
1148 GO enrichment analysis represented in blue and red bars. Annotation of putative coding
1149 genes was obtained using the blastx algorithm with *Arabidopsis thaliana* proteins as a
1150 reference; grey bars represent putative non-coding transcripts that are differentially
1151 expressed, and black bars represent putative coding transcripts that are differentially
1152 expressed but not annotated. (I-L) Examples of Gene Ontology (GO) terms enriched among
1153 overexpressed transcripts (DET) in Subtropical leaf samples; in Equatorial leaf samples; in
1154 Subtropical stem samples and in Equatorial stem samples. GO terms are ordered from the top
1155 down based on the P- value of enrichment (low to high, all < 0.05). Coloured bars represent
1156 the percentage of all DET that belong to each of the listed categories. Black bars represent the
1157 percentage of all transcripts in the reference transcriptome belonging to each category. Plant
1158 material of adult trees was sampled under field conditions, during the end of winter in the
1159 Subtropical site and in the beginning of the dry season in the Equatorial site. The complete
1160 lists of enriched GO terms are presented in S5-S8 Tables.
1161
1162 **S7 Fig. Validation of RNA-Sequencing-based differential expression of transcripts by**
1163 **reverse transcription real time PCR (qRT-PCR).** Each bar represents the relative
1164 expression of one sequenced sample. Error bars represent the standard deviation of the mean
1165 from three technical replicates of the same individual sample. Red bars represent samples
1166 from the Equatorial sampling site and blue bars, samples from the Subtropical sampling site.

Non-parametric unpaired Mann-Whitney Wilcoxon U-tests were used to compare the distributions. The differential expression detected *in silico* was confirmed *in vitro* for all putative genes, at a significance threshold of 0.05. Putative genes selected for the validation of the RNA-Seq data and primers sequences are described in S10 Table.

S8 Fig. Population structure of *A. schaueriana,* inferred from genome-wide genotyping of single nucleotide polymorphic (SNP) loci. (A) Density of individuals on the discriminant function, calculated using a multivariate method, the discriminant analysis of principal components (DAPC); different colours represent different inferred populations; (B) map showing the distribution of the species (green shaded area), the geographical location of sampling sites (points) and barplots in which each colour denotes an ancestral cluster and each line represents an individual as inferred by the method implemented in Admixture 1.3.0.

S9 Fig. Environmental data in the glasshouse and at the source sites of propagules used in the common-garden experiment. Green line: glasshouse; red line: Equatorial site (Tracuateua automatic station, source: Brazilian National Institute of Meteorology (INMET)); blue line: Subtropical site (Santa Marta automatic station, source: INMET). Multiple comparisons of periodic data of each environmental variable measured during the experiment were performed using ANOVA and post-hoc Tukey HSD tests with a significance threshold of 0.05. * represents significant difference and hyphen (-) represents an absence of a significant difference. (A) Average temperature; (B) average maximum temperature; (C) average minimum temperature; (D) average air humidity; (E) average air vapour pressure deficit (VPD).

S1 Table. Morphological traits analysed in *Avicennia schaueriana* saplings from Equatorial and Subtropical sites, grown under the same environmental conditions in a glasshouse.

S2 Table. Transcriptome quality parameters assessed in this work.

S3 Table. Transcriptome size characterisation.

S4 Table. Putative orthologous expressed sequences between the *Avicennia schaueriana* transcriptome sequenced in this work and publicly available transcriptomes from other congeneric.

S5 Table. Enriched Gene Ontology (GO) terms among differentially expressed transcripts (DET) that presented higher expression in Subtropical stem samples than in Equatorial stem samples.

S6 Table. Enriched Gene Ontology (GO) terms among differentially expressed transcripts (DET) that presented higher expression in Equatorial stem samples than in Subtropical stem samples.

S7 Table. Enriched Gene Ontology (GO) terms among differentially expressed transcripts (DET) that presented higher expression in Subtropical leaf samples than in Equatorial leaf samples.

S8 Table. Enriched Gene Ontology (GO) terms among differentially expressed transcripts (DET) that presented higher expression in Equatorial leaf samples than in Subtropical leaf samples.

S9 Table. Differentially expressed transcripts of *Avicennia schaueriana* involved in the response to contrasting climate conditions between Equatorial and Subtropical sites.

S10 Table. Oligonucleotides used in qRT-PCR reactions in this work.

S11 Table. Sampling sites for plant material used in nextRAD sequencing.

S12 Table. Single Nucleotide Polymorphic loci (SNP) with signature of selection present in putative protein-coding regions of the genome of *Avicennia schaueriana*.

S1 Method. Propagules and RNA sampling sites characterization.

S2 Method. RNA-sequencing data verification through qRT-PCR.

S1 Result. Validation of RNA-Seq data through qRT-PCR.

S1 Data. Morphological traits analysed in *Avicennia schaueriana* saplings from Equatorial and Subtropical sites, grown under the same environmental conditions in a glasshouse.

S2 Data. Stem light reflectance data.

S3 Data. Variant Call Format (VCF) file required for all genome-wide SNP diversity analyses.

S4 Data. Text file complementary to S3 Data file required for all genome-wide SNP diversity analyses.